

DAFTAR PUSTAKA

- Achmad, T. L. (2021). *Grand Strategy Mineral dan Batubara*. Jakarta: Direktorat Jenderal Mineral dan Batubara Kementerian Energi dan Sumber Daya Mineral.
- Anbiyak, N., & Cahyaningrum, T. (2021). Identifikasi Zona Kaya Kobalt Pada Cebakan Nikel Laterit di Indonesia. *Indonesian Mining Professionals Journal*, 2(2), pp. 103-110.
- Arista, S., Sari, R. P., & Liony, I. (2015). Purifikasi Limbah Spent Acid Dengan Proses Adsorpsi Menggunakan Zeolit dan Bentonit. *Jurnal Teknik Kimia*, 21(4), pp. 65-72.
- Asadrokht, M., & Zakeri, A. (2022). Chemo-Physical Concentration of a Low-Grade Nickel Laterite Ore. *Minerals Engineering*, 178, pp. 1-8.
- Arif, I. (2018). *Nikel Indonesia*. Jakarta: PT Gramedia Pustaka Utama.
- Astuti, W., Mufakhir, F. R., Nurjaman, F., Sumardi, S., Herlina, U., Bahfie, F., Petrus, H. T. B. M. (2021). Pengaruh Karakteristik Bijih Pada Ekstraksi Nikel dari Bijih Limonit Indonesia Menggunakan Pelindian Atmosferik. *Jurnal Metal Indonesia (JMI)*, 43(1), pp. 9-16.
- Astuti, W., Nurjaman, F., Mufakhir, F. R., Sumardi, S., Avista, D., Wanta, K. C., & Petrus, H. T. B. M. (2023). A Novel Method: Nickel and Cobalt Extraction from Citric Acid Leaching Solution of Nickel Laterite Ores Using Oxalate Precipitation. *Minerals Engineering*, 191, pp. 1-6.
- Bahfie, F., Manaf, A., Astuti, W., Nurjaman, F., & Herlina, U. (2021). Tinjauan Teknologi Proses Ekstraksi Bijih Nikel Laterit. *Jurnal Teknologi Mineral dan Batubara*, 17(3), pp. 135-152.
- Bakri, S., & Sanwani, E. (2019). Studi Transformasi Goetit Menjadi Hematit Secara Mekanokimia Untuk Benefisiasi Bijih Besi Laterit. *Jurnal Teknologi Mineral dan Batubara*, 15(3), pp. 179-188.
- Basturkcu, H., & Acarkan, N. (2016). Separation Of Nickel and Iron from Lateritic Ore Using a Digestion - Roasting - Leaching - Precipitation Process. *Physicochemical Problems of Mineral Processing*, 52(2), pp. 564-574.
- Bunjaku, A., Kekkonen, M., & Holappa, L. (2010). Phenomena in Thermal Treatment of Lateritic Nickel Ores up to 1300°C. *12th International Ferroalloys Congress*, pp. 641-652.

- Celep, O., Alp, I., & Deveci, H. (2010). The Application of Roasting Pretreatment for Antimonial Refractory Gold and Silver Ores. *XXV International Mineral Processing Congress (IMPC) 2010 Proceedings*, pp. 1505-1510.
- Dahani, W., Jaksa, I. G. N. B. S., Marwanza, I., Kurniawati, R., & Subandrio, S. (2020). The Effect of Pre-roasting on Nickel Extraction from Limonite Ore by Acid Leaching Method. *AIP Conference Proceedings*, 2267, pp. 1-4.
- Dalvi, A. D., Bacon, W. G., & Osborne, R. C. (2004). The Past and The Future of Nickel Laterites. In: *PDAC 2004 International Convention, Trade Show & Investors Exchange*, pp. 1-27.
- Dehaine, Q., Tijsseling, L. T., Glass, H. J., Tormanen, T., & Butcher, A. R. (2021). Geometallurgy of Cobalt Ores: A Review. *Minerals Engineering*, 160, pp. 1-128.
- Dong, B., Tian, Q., Xu, Z., Wang, Q., & Li, D. (2023). The Effect of Pre-roasting on Atmospheric Sulfuric Acid Leaching of Saprolitic Laterites. *Hydrometallurgy*, 218, pp. 1-8.
- Elias, M. (2002). *Nickel Laterite Deposits - Geological Overview, Resources and Exploitation*. Burswood: CSA Australia Pty Ltd.
- Fan, R., & Gerson, A. R. (2013). Mineralogical Characterisation of Indonesian Laterites Prior to and Post Atmospheric Leaching. *Hydrometallurgy*, 134-135, pp. 102-109.
- Fathoni, M. W., & Mubarok, M. Z. (2015). Studi Perilaku Pelindian Bijih Besi Nikel Limonit dari Pulau Halmahera Dalam Larutan Asam Nitrat. *Majalah Metalurgi*, 30(3), pp. 115-124.
- Fatimah, S. (2018). *Identifikasi Kandungan Unsur Logam Menggunakan XRF dan OES Sebagai Penentu Tingkat Kekerasan Baja Paduan*. Yogyakarta: Universitas Negeri Yogyakarta.
- Febriana, E., Tristiyan, A., Mayangsari, W., & Prasetyo, A. B. (2018). Kinetika dan Mekanisme Pelindian Nikel dari Bijih Limonit: Pengaruh Waktu dan Temperatur. *Majalah Metalurgi*, 33(2), pp. 61-68.
- Garces-Granda, A., Lapidus, G.T., & Restrepo-Baena, O.J. (2020). Effect of a Thermal Pretreatment on Dissolution Kinetics of a Limonitic Laterite Ore in Chloride Media. *Hydrometallurgy*, 196, pp. 1-7.
- Hardani., Andriani, H., Ustiawaty, J., Utami, E. F., Istiqomah, R. R., Fardani, R. A., Sukmana, D. J., & Auliya, N. H. (2020). *Metode Penelitian Kualitatif & Kuantitatif*. Yogyakarta: CV. Pustaka Ilmu Group.

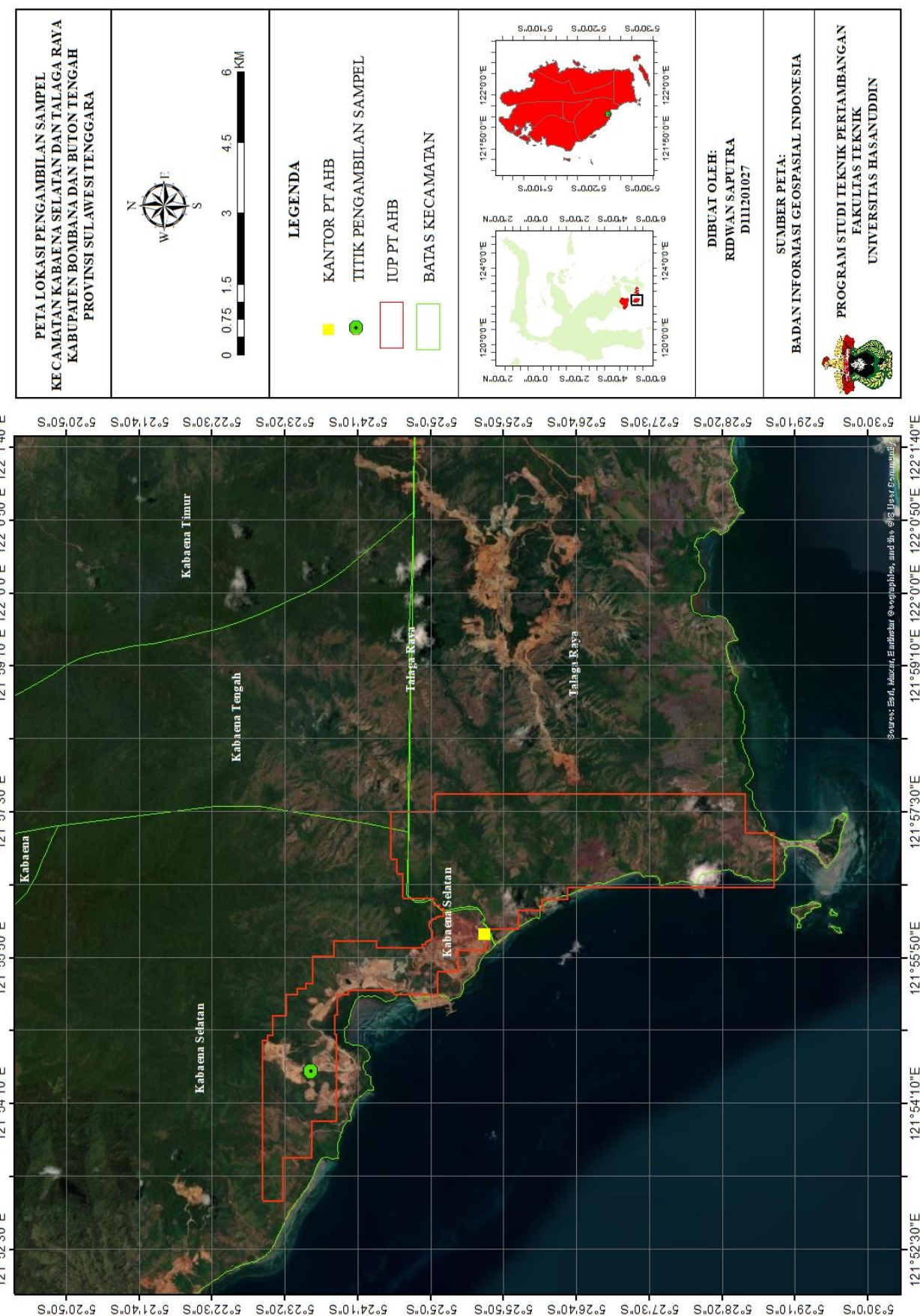
- Hariyanto, R. K. S., Rocha, L. T. D., Kim, S. J., & Jung, S. M. (2023). Extraction Behavior of Nickel and Cobalt from Serpentine - Rich Ore Through Sulfation - Roasting - Leaching Process. *Metallurgical And Materials Transactions*, 54, pp. 2915-2928.
- He, F., Ma, B., Qiu, Z., Wang, C., Chen, Y., & Hu, X. (2023). Enhanced Extraction of Nickel from Limonitic Laterite Via Improved Nitric Acid Pressure Leaching Process. *Minerals Engineering*, 201, pp. 1-10.
- Kurniadi, A., Rosana, M. F., Yuningsih, E. T., & Pambudi, L. (2018). Karakteristik Batuan Asal Pembentukan Endapan Nikel Laterit di Daerah Madang dan Serakaman Tengah. *Padjadjaran Geoscience Journal*, 2(3), pp. 221-234.
- Li, J., Li, X., Hu, Q., Wang, Z., Zhou, Y., Zheng, J., Liu, W., & Li, L. (2009). Effect of Pre-Roasting on Leaching of Laterite. *Hydrometallurgy*, 99, pp. 84-88.
- Liu, H., Chen, T., Chang, J., Zou, X., & Frost, R. L. (2013). The Effect of Hydroxyl Groups and Surface Area of Hematite Derived from Annealing Goethite for Phosphate Removal. *Journal of Colloid and Interface Science*, 398, pp. 88-94.
- Maharani, R. A. S., & Muin, Z. (2023). Teknologi Hijau Pengelolaan Bijih Nikel Laterit. *JUTIN: Jurnal Teknik Industri Terintegrasi*, 6(3), pp. 661-678.
- Masri, Mili, M. Z., Nafiu, W. R. A., Tugo, L. J., & Rifai, L. O. A. (2023). Mineralogi dan Properti Keteknikan Endapan Nikel Laterit Daerah Tobimeita - Langgikima, Kabupaten Konawe Utara, Sulawesi Tenggara. *Jurnal GEOSAPTA*, 9(2), pp. 117-125.
- McDonald, R. G., & Whittington, B. I. (2008). Atmospheric Acid Leaching of Nickel Laterites Review Part I. Sulphuric Acid Technologies. *Hydrometallurgy*, 91, pp. 35-55.
- Mohammadreza, F., Mohammad, N., & Ziaeddin, S. S. (2014). Nickel Extraction From Low Grade Laterite by Agitation Leaching at Atmospheric Pressure. *International Journal of Mining Science and Technology*, 24(4), pp. 543-548.
- Mukhtar, M., Arninda, A., & Diana, S. (2022). Pengaruh Konsentrasi HCL Terhadap Persen Recovery Nikel Laterit Pada Proses Pelindian. *Prosiding Seminar Nasional Teknologi Industri IX*, 9(1), pp. 185-188.
- Nurfaidah, A. N., Lestari, D. P., Azzahra, R. T., & Suminar, D. R. (2020). Kajian Pustaka Pengaruh Suhu dan Konsentrasi Terhadap Proses Pemisahan Nikel dari Logam Pengotor Menggunakan Metode Leaching. *Jurnal Fluida*, 13(2), pp. 81-92.

- Okto, A., Bahdad., Razak, S., Sahiddin., & Tugo, J. (2023). Pengkayaan Unsur Logam Tanah Jarang Kobalt (Co) Pada Profil Laterit di Kecamatan Kolaka Utara. *Jurnal GEOSAPTA*, 9(2), pp. 127-135.
- Park, J. O., Kim, H. S., & Jung, S. M. (2015). Use of Oxidation Roasting to Control NiO Reduction in Ni-Bearing Limonitic Laterite. *Minerals Engineering*, 71, pp. 205-215.
- Petavratzi, E., Gunn, G., & Kresse, C. (2019). *Commodity Review: Cobalt*. Nottingham: British Geological Survey.
- Prameswara, G. (2023). Perilaku Leaching dari Roasted Laterite Ore Dalam Peningkatan Rekoveri Logam. *Jurnal Teknologi Kimia Mineral*, 2(2), pp. 60-64.
- Prasetyo, P. (2016). Tidak Sederhana Mewujudkan Industri Pengolahan Nikel Laterit Kadar Rendah di Indonesia Sehubungan Dengan Undang Undang Minerba 2009. *Jurnal Teknologi Mineral dan Batubara*, 12(3), pp. 195-207.
- Ribeiro, P. P. M., Souza, L. C. M. D., Neumann, R., Santos, I. D. D., & Dutra, A. J. B. (2020). Nickel and Cobalt Losses from Laterite Ore After The Sulfation - Roasting - Leaching Processing. *Journal of Materials Research and Technology*, 9(6), pp. 12404-12415.
- Ridha, N. (2017). Proses Penelitian, Masalah, Variabel dan Paradigma Penelitian, *Jurnal Hikmah*, 14(1), pp. 62-70.
- Rodrigues, F. M. (2013). *Investigation Into The Thermal Upgrading of Nickeliferous Laterite Ore*. Kingston: Queen's University.
- Solihin., & Firdiyono, F. (2018). Perilaku Pelarutan Logam Nikel dan Besi dari Bijih Nikel Kadar Rendah Sulawesi Tenggara. *Majalah Metalurgi*, 29(2), pp. 139-144.
- Sufriadin. (2013). *Mineralogi, Geokimia dan Sifat "Leaching" Pada Endapan Laterit Nikel Soroako, Sulawesi Selatan, Indonesia*. Yogyakarta: Universitas Gadjah Mada.
- Sufriadin, Widodo, S., Nur, I., Ilyas, A., & Ashari, M. Y. (2020). Extraction of Nickel and Cobalt from Sulawesi Limonite Ore in Nitric Acid Solution at Atmospheric Pressure. *IOP Conf. Series: Materials Science and Engineering*, 875, pp. 1-6.
- Suhaimi, L., & Indrawati, E. (2022). Pelindian Nikel Laterit Low - Grade Pomala Menggunakan Asam Organik dan Asam Inorganik Pada Kondisi Atmosfir. *HEXAGON (Jurnal Teknik dan Sains)*, 3(2), pp. 8-12.

- Taylor, G., & Eggleton, R. A. (2001). *Regolith Geology and Geomorphology*. New York: John Wiley & Sons.
- Ulfa, R. (2021). Variabel Penelitian Dalam Penelitian Pendidikan. *Al-Fathonah: Jurnal Pendidikan dan Keislaman*, 1(1), pp. 342-351.
- Wahab., Anshari, E., Mili, M. Z., Nafiu, W. R. A., Khaq, M. N., Deniyatno., Firdaus., & Supriyatna, Y. I. (2021). Studi Pengaruh Variabel Proses dan Kinetika Ekstraksi Nikel dari Bijih Nikel Laterit Menggunakan Larutan Asam Sulfat Pada Tekanan Atmosferik. *Jurnal Rekayasa Proses*, 15 (1), pp. 37-48.
- Wahab., Deniyatno., Ismayanti, W., & Supriatna, Y. I. (2021). Pengaruh Variabel Pelindian Terhadap Ekstraksi Nikel Dalam Pelindian Bijih Nikel Laterit. *Jurnal Sains dan Teknologi*, 10(2), pp. 127-134.
- Wahyuni, M. (2020). *Statistik Deskriptif Untuk Penelitian Olah Data Manual dan SPSS Versi 25*. Yogyakarta: Bintang Pustaka Madani.
- Werling, N., Kaltenbach, J., Weidler, P. G., Schuhmann, R., Dehn, F., & Emmerich, K. (2022). Solubility of Calcined Kaolinite, Montmorillonite, and Illite in High Molar NaOH and Suitability as Precursors for Geopolymers. *Clays Clay Miner*, 70(2), pp. 270-289.
- Whittington, B. I., & Muir, D. (2000). Pressure Acid Leaching of Nickel Laterites: A Review. *Mineral Processing and Extractive Metallurgy Review*, 21(6), pp. 527-599.
- Wulandari, W., Soerawidjaja, T. H., Alifiani, D., & Rangga, D. A. (2017). The Effect of Pre-Treatments to The Nickel Limonite Leaching Using Dissolved Gaseous SO₂ - Air. *IOP Conference Series: Materials Science and Engineering*, 285, pp. 1-6.
- Yanuar, E., Alkaf, S. M. A., & Bahtiar, S. (2024). Pengaruh Jenis Asam & Konsentrasi Asam Terhadap Persentase Ekstraksi Nikel dari Bijih Nikel Laterit Pomalaa Sulawesi Tenggara. *HEXAGON (Jurnal Teknik dan Sains)*, 5(1), pp. 32-41.
- Zhao, Z., Li, H., Wang, C., & Xing, P. (2024). Transformation Mechanism and Selective Leaching of Nickel and Cobalt From Limonitic Laterite Ore Using Sulfation - Roasting - Leaching Process. *Journal of Cleaner Production*, 445, pp. 1-10.
- Ziwa, G., Crane, R., & Edwards, K. A. H. (2021). Geochemistry, Mineralogy and Microbiology of Cobalt in Mining - Affected Environments. *Minerals*, 11(22), pp. 1-20.

LAMPIRAN

LAMPIRAN 1
PETA LOKASI PENGAMBILAN SAMPEL



LAMPIRAN 2**PERHITUNGAN PENGENCERAN ASAM SULFAT (H_2SO_4) 98%**

Densitas	= 1,83 g/mL
Massa molekul relatif (Mr)	= 98 g/mL
V larutan	= 1000 mL
% larutan	= 98%

$$\text{Molaritas (M)} = \frac{\% \text{massa} \times \text{densitas} \times V}{\text{Mr}}$$

$$= \frac{98\% \times 1,83 \frac{\text{g}}{\text{mL}} \times 1000 \text{ mL}}{98 \text{ g/mL}}$$

$$= 18,3$$

$$M_1 V_1 = M_2 V_2$$

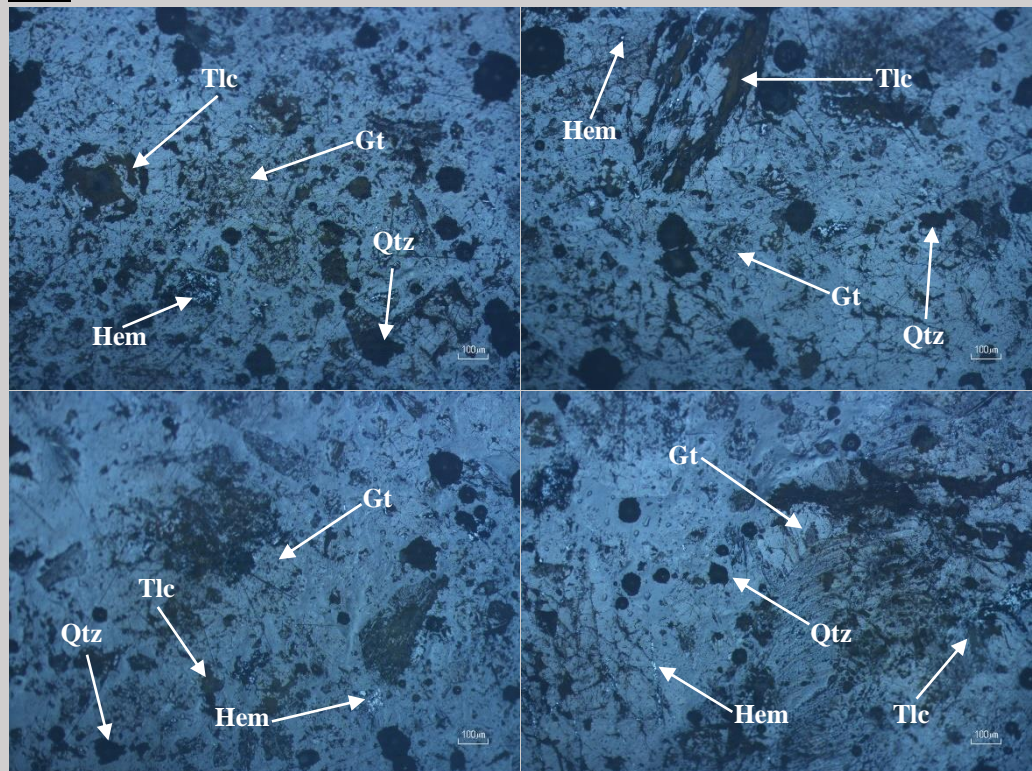
$$18,3 \times V_1 = 2 \times 1000 \text{ mL}$$

$$V_1 = \frac{2 \times 1000 \text{ mL}}{18,3}$$

$$= 109,29 \text{ mL}$$

$$\approx 109 \text{ mL}$$

LAMPIRAN 3
HASIL ANALISIS MIKROSKOPIS

Lokasi: Blok A1-07 PT Anugrah Harisma Barakah (Pulau Kabaena)
Foto

Lensa Okuler: 10x
Lensa Objektif: 10x
Pembesaran Total: 100x
Tipe Endapan: Nikel laterit
Jenis Mineralisasi: Quartz - Talc - Goethite - Hematit
Referensi: : Ore Mineral Atlas (Marshall, 2004)

Mikroskopis:

Kenampakan bijih limonit dalam bentuk sayatan poles berdasarkan pengamatan mikroskop memperlihatkan mineral yang terdiri dari *quartz*, *talc*, *goethite*, dan *hematite*.

Deskripsi Mineralogi

Komposisi Mineral	Simbol	Keterangan Optik Mineral
<i>Quartz</i> (SiO_2)	Qtz	Berwarna hitam, bentuk kristal <i>anhedral</i> , dan ukuran mineral 50-100 μm .
<i>Talc</i> ($\text{Mg}_3\text{Si}_4\text{O}_{10}(\text{OH})_2$)	Tlc	Berwarna cokelat, bentuk <i>anhedral-subhedral</i> , dan ukuran mineral 50-150 μm .
<i>Goethite</i> ($\text{FeO}(\text{OH})$)	Gt	Berwarna putih keabu-abuan, bentuk kristal <i>anhedral-subhedral</i> , dan ukuran mineral 50-300 μm .
<i>Hematite</i> (Fe_2O_3)	Hem	Berwarna putih, bentuk kristal <i>anhedral-subhedral</i> , dan ukuran mineral 20-40 μm .

LAMPIRAN 4
HASIL ANALISIS X-RAY FLUORESCENCE (XRF)

Sample ID	Measurement method	Measurement Finished	Ni (%)	Fe ₂ O ₃ (%)	MgO (%)	SiO ₂ (%)	Al ₂ O ₃ (%)	CaO (%)	Co (%)	Cr ₂ O ₃ (%)	MnO (%)	Fe (%)
TA-RS LIM 01	LAB AHB2023	20/01/2024 13:10	1.66	26.91	4.42	42.33	3.71	0.12	0.06	1.13	0.37	18.82
TA-RS LIM 02	LAB AHB2023	20/01/2024 13:14	1.68	26.97	4.54	42	3.94	0.13	0.06	1.12	0.37	18.86
Rata-Rata			1.67	26.94	4.48	42.17	3.83	0.13	0.06	1.13	0.37	18.84

LAMPIRAN 5

**HASIL ANALISIS *ATOMIC ABSORPTION SPECTROPHOTOMETRY*
(AAS)**



PT. AISPEKTRA LABORATORY SERVICES

Office : Kompleks Komplek Puri Residence Blok D/7
Jl Tamalanrea Raya, Makassar 90245 Sulawesi Selatan
Telp/Fax. +62 4118994478 Email : info@aispektra.co.id

REPORT OF ANALYSIS (Laporan Analisis)

Certificate Number/Nomor Sertifikat	: 000422024
Customer/Pelanggan	: RIDWAN
Subject / Hal	: Mineral Analysis
Description of Sample/ Keterangan Sampel	: Nickel Ore
Number of Sample (s) / Jumlah Sampel	: 7 (Seven)
Form of Sample / Bentuk Sampel	: Solid & Liquid
Test Required / Analisa uji	: Elemental (Ni, Co)
Date Received/ Tanggal terima	: 20/06/2024
Date of Analysis / Tanggal Analisa	: 26/06/2024
Method of Analysis/ Metode analisa	: AAS
Reference / Referensi	: -

RESULT

SAMPLE ID	Ni (mg/L)	Co (mg/L)	Fe (mg/L)	Al (mg/L)	Remarks
SA	15562.25	630.79	NA	NA	
T100	909.87	11.69752	NA	NA	
T200	994.56	13.25784	NA	NA	
T300	900.54	11.16512	NA	NA	
T400	897.08	9.54368	NA	NA	
T500	1018.37	13.36904	NA	NA	
T600	1121.90	13.27824	NA	NA	

Note : NA = Not Analyzed

HASIL ANALISA TERSEBUT DIATAS HANYA MERUJUK PADA SAMPEL YANG DISERAHKAN
DIMANA PENGAMBILAN SAMPEL TERSEBUT TIDAK DILAKUKAN OLEH AISPEKTRA
LABORATORY

ANALIS



FAJRIN AHMAD, A.Ma

LAMPIRAN 6
PERHITUNGAN TINGKAT PELINDIAN

Tingkat pelindian Ni dan Co pada penelitian ini dihitung menggunakan rumus efisiensi pelindian dalam Dong *et al.* (2023) pada Persamaan 3 berikut ini.

$$\eta = \frac{C_i \times V}{m \times W_i} \times 100\%$$

Dimana:

η = Tingkat pelindian (%)

C_i = Konsentrasi logam (mg/L) dalam *Pregnant Leach Solution* (PLS)

V = Volume PLS (L)

m = Massa sampel (Kg)

W_i = Kadar logam (mg/Kg)

TINGKAT PELINDIAN NIKEL (Ni)

Volume PLS (V) = 0,075 L

Massa sampel (m) = 0,01 Kg

Kadar Nikel (W_i) = 15562,25 mg/Kg

1. Tingkat Pelindian Nikel 100°C ($C_i = 909,87$ mg/L)

$$\begin{aligned}\text{Tingkat Pelindian (\%)} &= \frac{C_i \times V}{m \times W_i} \times 100\% \\ &= \frac{909,87 \times 0,075}{0,01 \times 15562,25} \times 100\% \\ &= 43,85\%\end{aligned}$$

2. Tingkat Pelindian Nikel 200°C ($C_i = 994,56$ mg/L)

$$\begin{aligned}\text{Tingkat Pelindian (\%)} &= \frac{C_i \times V}{m \times W_i} \times 100\% \\ &= \frac{994,56 \times 0,075}{0,01 \times 15562,25} \times 100\% \\ &= 47,93\%\end{aligned}$$

3. Tingkat Pelindian Nikel 300°C ($C_i = 900,54$ mg/L)

$$\text{Tingkat Pelindian (\%)} = \frac{C_i \times V}{m \times W_i} \times 100\%$$

$$\begin{aligned}
 &= \frac{900,54 \times 0,075}{0,01 \times 15562,25} \times 100\% \\
 &= 43,40\%
 \end{aligned}$$

4. Tingkat Pelindian Nikel 400°C ($C_i = 897,08 \text{ mg/L}$)

$$\begin{aligned}
 \text{Tingkat Pelindian (\%)} &= \frac{C_i \times V}{m \times W_i} \times 100\% \\
 &= \frac{897,08 \times 0,075}{0,01 \times 15562,25} \times 100\% \\
 &= 43,23\%
 \end{aligned}$$

5. Tingkat Pelindian Nikel 500°C ($C_i = 1018,37 \text{ mg/L}$)

$$\begin{aligned}
 \text{Tingkat Pelindian (\%)} &= \frac{C_i \times V}{m \times W_i} \times 100\% \\
 &= \frac{1018,37 \times 0,075}{0,01 \times 15562,25} \times 100\% \\
 &= 49,08\%
 \end{aligned}$$

6. Tingkat Pelindian Nikel 600°C ($C_i = 1121,90 \text{ mg/L}$)

$$\begin{aligned}
 \text{Tingkat Pelindian (\%)} &= \frac{C_i \times V}{m \times W_i} \times 100\% \\
 &= \frac{1121,90 \times 0,075}{0,01 \times 15562,25} \times 100\% \\
 &= 54,07\%
 \end{aligned}$$

TINGKAT PELINDIAN KOBALT (Co)

Volume PLS (V) = 0,075 L

Massa sampel (m) = 0,01 Kg

Kadar Kobalt (W_i) = 630,79 mg/Kg

1. Tingkat Pelindian Kobalt 100°C ($C_i = 11,69752 \text{ mg/L}$)

$$\text{Tingkat Pelindian (\%)} = \frac{C_i \times V}{m \times W_i} \times 100\%$$

$$\begin{aligned}
 &= \frac{11,69752 \times 0,075}{0,01 \times 630,79} \times 100\% \\
 &= 13,91\%
 \end{aligned}$$

2. Tingkat Pelindian Kobalt 200°C ($C_i = 13,25784$ mg/L)

$$\begin{aligned}
 \text{Tingkat Pelindian (\%)} &= \frac{C_i \times V}{m \times W_i} \times 100\% \\
 &= \frac{13,25784 \times 0,075}{0,01 \times 630,79} \times 100\% \\
 &= 15,76\%
 \end{aligned}$$

3. Tingkat Pelindian Kobalt 300°C ($C_i = 11,16512$ mg/L)

$$\begin{aligned}
 \text{Tingkat Pelindian (\%)} &= \frac{C_i \times V}{m \times W_i} \times 100\% \\
 &= \frac{11,16512 \times 0,075}{0,01 \times 630,79} \times 100\% \\
 &= 13,28\%
 \end{aligned}$$

4. Tingkat Pelindian Kobalt 400°C ($C_i = 9,54368$ mg/L)

$$\begin{aligned}
 \text{Tingkat Pelindian (\%)} &= \frac{C_i \times V}{m \times W_i} \times 100\% \\
 &= \frac{9,54368 \times 0,075}{0,01 \times 630,79} \times 100\% \\
 &= 11,35\%
 \end{aligned}$$

5. Tingkat Pelindian Kobalt 500°C ($C_i = 13,36904$ mg/L)

$$\begin{aligned}
 \text{Tingkat Pelindian (\%)} &= \frac{C_i \times V}{m \times W_i} \times 100\% \\
 &= \frac{13,36904 \times 0,075}{0,01 \times 630,79} \times 100\% \\
 &= 15,90\%
 \end{aligned}$$

6. Tingkat Pelindian Kobalt 600°C ($C_i = 13,27824 \text{ mg/L}$)

$$\begin{aligned}\text{Tingkat Pelindian (\%)} &= \frac{C_i \times V}{m \times W_i} \times 100\% \\ &= \frac{13,27824 \times 0,075}{0,01 \times 630,79} \times 100\% \\ &= 15,79\%\end{aligned}$$

LAMPIRAN 7

HASIL ANALISIS X-RAY DIFFRACTION (XRD)

Match! Phase Analysis Report

Sample: RIDWAN-SAMPEL-AWAL

Sample Data

File name	RIDWAN-SAMPEL-AWAL.txt
File path	D:/TUGAS AKHIR (TA)/HASIL ANALISIS DAN PENGOLAHAN DATA/HASIL ANALISIS/ANALISIS XRD 2/RIDWAN-SAMPEL-AWAL
Data collected	Aug 5, 2024 23:16:18
Data range	5.000° - 70.000°
Original data range	5.000° - 70.000°
Number of points	3251
Step size	0.020
Rietveld refinement converged	No
Alpha2 subtracted	No
Background subtr.	No
Data smoothed	Yes
Radiation	X-rays
Wavelength	1.541874 Å

Matched Phases

Index	Amount (%)	Name
A	59.4	Quartz
B	23.3	Talc
C	9.1	Goethite
D	3.8	Lizardite
E	2.5	Montmorillonite
F	1.9	Gibbsite
	6.9	Unidentified peak area

Formula sum
O2 Si
H2 Mg3 O12 Si4
Fe H O2
H4 Mg3 O9 Si2
Al2 Ca O12 Si4
Al O3

A: Quartz (59.4 %)

Formula sum	O2 Si
Entry number	96-901-2601
Figure-of-Merit (FoM)	0.864417
Total number of peaks	70
Peaks in range	36
Peaks matched	26
Intensity scale factor	0.77
Space group	P 31 2 1
Crystal system	trigonal (hexagonal axes)
Unit cell	a= 4.9140 Å c= 5.4060 Å
I/c	3.32
Calc. density	2.648 g/cm³
Reference	Hazen R. M., Finger L. W., Hemley R. J., Mao H. K., "High-pressure crystal chemistry and amorphization of alpha-quartzLocality: syntheticSample: P = 1 bar", Solid State Communications 72 , 507-511 (1989)

B: Talc (23.3 %)

Formula sum	H2 Mg3 O12 Si4
Entry number	96-900-8041
Figure-of-Merit (FoM)	0.508953
Total number of peaks	596
Peaks in range	359
Peaks matched	79
Intensity scale factor	0.11
Space group	C 1 2/c 1
Crystal system	monoclinic
Unit cell	a= 5.2600 Å b= 9.1000 Å c= 18.8100 Å β= 100.000 °
I/c	1.23
Calc. density	2.841 g/cm³
Reference	Gruner J. W., "The crystal structures of talc and pyrophylliteLocality: Harford County, Maryland, USA", Zeitschrift fur Kristallographie 88 , 412-419 (1934)

C: Goethite (9.1 %)

Formula sum	Fe H O2
Entry number	96-900-2160
Figure-of-Merit (FoM)	0.481317
Total number of peaks	172
Peaks in range	72
Peaks matched	27
Intensity scale factor	0.10
Space group	P n m a
Crystal system	orthorhombic
Unit cell	a= 9.9189 Å b= 3.0148 Å c= 4.5835 Å
I/c	2.72
Calc. density	4.306 g/cm³
Reference	Gualtieri A., Venturelli P., "In situ study of the goethite-hematite phase transformation by real timesynchrotron powder diffractionSample at T = 156 C", American Mineralogist 84 , 895-904 (1999)

D: Lizardite (3.8 %)

Formula sum	H4 Mg3 O9 Si2
Entry number	96-900-7425
Figure-of-Merit (FoM)	0.305135
Total number of peaks	118
Peaks in range	55
Peaks matched	19
Intensity scale factor	0.02
Space group	P 1

Crystal system	triclinic (anorthic)
Unit cell	$a=5.4340 \text{ \AA} b=5.4340 \text{ \AA} c=7.1530 \text{ \AA} \alpha=90.000^\circ \beta=90.000^\circ \gamma=120.000^\circ$
I/c	1.22
Calc. density	2.516 g/cm ³
Reference	Auzende A. L., Pellenq R. J. M., Devouard B., Baronnet A., Grauby O., "Atomistic calculations of structural and elastic properties of serpentine minerals: the case of lizardite Note: 1T polytype Note: Hypothetical structure derived using semi-empirical potentials", Physics and Chemistry of Minerals 33, 266-275 (2006)

E: Montmorillonite (2.5 %)

Formula sum	Al2 Ca O12 Si4
Entry number	96-110-1055
Figure-of-Merit (FoM)	0.571725
Total number of peaks	184
Peaks in range	184
Peaks matched	34
Intensity scale factor	0.20
Space group	P 1
Crystal system	triclinic (anorthic)
Unit cell	$a=5.1800 \text{ \AA} b=8.9800 \text{ \AA} c=15.0000 \text{ \AA} \alpha=90.000^\circ \beta=90.000^\circ \gamma=90.000^\circ$
I/c	20.57
Calc. density	1.800 g/cm ³

F: Gibbsite (1.9 %)

Formula sum	Al O3
Entry number	96-901-5977
Figure-of-Merit (FoM)	0.491155
Total number of peaks	860
Peaks in range	342
Peaks matched	52
Intensity scale factor	0.02
Space group	P 1 21/n 1
Crystal system	monoclinic
Unit cell	$a=8.6410 \text{ \AA} b=5.0700 \text{ \AA} c=9.7200 \text{ \AA} \beta=85.430^\circ$
I/c	2.06
Calc. density	2.347 g/cm ³
Reference	Megaw H., "The crystal structure of Hydargillite Al(OH)3 cod_database_code 1011081", Zeitschrift fur Kristallographie 87, 185-204 (1934)

Candidates

Name	Formula	Entry No.	FoM
Cd32 Cs28 (Al92 Si100 O384)	C48 H156 As2 Cl6 Mn6 N12 O72 W18	96-432-8916	0.7211
catena-(1,8-Octanediammonium (l-m~2~-fluoro)-tetrafluoro-aluminium)	A92 Cd32 Cs28 O384 Si100	96-153-1645	0.7196
S19 (Sb F6)2	C8 H22 Al F5 N2	96-110-0116	0.7157
((libiox12)PdCl2)2 hexane sovate	C12 Cu2 O7 P2	96-431-1828	0.7145
Ni20 ((O H)12 (H2 O)6) (H P O4)8 (P O4)4 (H2 O)12.35	H172 K6 Na4 Nd12 O410 Sm12 W87	96-704-4074	0.7121
[V(IV)O(BPDC)]	C48 H156 Cl6 Cu6 N12 O72 Sb2 W18	96-432-8915	0.7100
CIS-11	F12 S19 Sb2	96-202-0229	0.7098
DMOF-1-bpdc-NO2	C18 Cr3 O38.33 P0.33 W4	96-433-8038	0.7097
(N H3)134.6 (Ca46 (Si100 Al92 O384))	C37 H90 Ca Cl Cu6 N7 O50	96-154-9267	0.7081
Ag55.5 Al55.5 Si136.5 O384	H172 K6 Na4 Nd12 O410 W87	96-704-4076	0.7075
Pd14 (O H Pd O Pd O H)8 Na32 (Al92 Si100 O384)	C66 H14.75 Cl4 N4 O4 Pd2	96-411-3181	0.7055
La33.1 (H3 O)16 Al92 Si100 O384 (O H)23.3 (H2 O)143.9	Ce12 H172 K6 Na4 Nd12 O410 W87	96-704-4075	0.7023
Rb35.2 Na31.36 (Al96 Si96 O384) (H2 O)134.56	Ni56.7 Ni20 O78.35 P12	96-153-4812	0.6988
Na0.99 Ba46.32 Si98.37 Al93.63 O384 (D2 O)51.296	C14 O5 V	96-433-1627	0.6984
Pb49 Ti18 O17 (Si100 Al92 O384)	C24 H16 Ag5 N5 O15	96-403-0809	0.6982
Sm0.516 Sr0.94 Nb S3.5	C88 H220 Cu7 In28 N11 S53	96-410-2052	0.6966
Cs4.51 Na83.75 (Al88 Si104 O384) (H2 O)34.84	C36 H0 N2 O8 Zn2	96-721-4549	0.6952
Na7 Gd27 (Al88.11 Si103.9 O384) (H2 O)195	C14 H47 F Ge7.2 N4 O19.4	96-450-3702	0.6939
K66.56 Na21.66 (Al88 Si104 O384) (H2 O)7.137	A92 Ce46 H403.8 N134.6 O384 Si100	96-152-1233	0.6927
(La4 (Mo O4) (H2 O)16 (Mo7 O24)4) N1.33 O24.65 C5.33	C12 Mg N2 O14 P4	96-432-9708	0.6909
Li17.28 Na30.72 (Al92 Si100 O384) (H2 O)69.06	Ag0.64 Al55.5072 O384 Si136.493	96-152-4401	0.6881
Sr26.56 Si136.5 Al55.5 O384	C12 H10 O6 P2 Zr	96-210-1068	0.6854
Ag92 (Al92 Si100 O384) (H2 O)48	Nb S2	96-152-0920	0.6845
(Sr46 (Si100 Al92 O384)) (N H3)102	A92 H16 Na32 O408 Pd30 Si100	96-152-1496	0.6844
Na54 (D3 O)42 (Si96 Al96 O384) (D2 O)80	Er12 H172 K6 Na4 O410 W87	96-704-4078	0.6838
Cr4.2 Na74 (N O2)86 (Si O2)106 (H2 O)230	C29 I4 Mn7 O24	96-410-8211	0.6829
	C10 H10 C2 F2 N2 O8 P2	96-431-0851	0.6824
	A92 H359.1 La33.1 O567.2 Si100	96-152-1727	0.6821
	A96 H269.12 Na31.36 O518.56 Rb35.2 Si96	96-154-0966	0.6804
	A93.63 Ba46.32 D102.592 Na0.99 O435.296 Si98.3796-152-1760		0.6798
	A92 O401 Pb49 Si100 Ti18	96-152-2288	0.6791
	C65 H95 N7 O20 S6 Zn4	96-710-8808	0.6779
	C65 H95 N7 O20 S6 Zn4	96-711-2416	0.6779
	Nb S2	96-153-3482	0.6775
	C8 H9 Cd O4 P	96-432-6744	0.6761
	Cu17 Ga22 S88 Sn17	96-712-3375	0.6741
	C12 O7 P2 Zn	96-431-1830	0.6733
	Al88 Cs4.51 H69.68 Na83.75 O418.84 Si104	96-152-1410	0.6715
	C40 N20 O12 Pd4	96-431-4739	0.6705
	A88.11 Gd27 H390 Na7 O579 Si103.9	96-153-9659	0.6688
	A88 H14.274 K66.56 Na21.66 O391.137 Si104	96-152-1409	0.6674
	C5.33 H32 La4 Mo29 N1.33 O140.65	96-403-1604	0.6667
	A92 H138.12 Li17.28 Na30.72 O453.06 Si100	96-154-0962	0.6661
	O4 S20 Sn10	96-155-0918	0.6660
	A55.5 O384 Si136.5 Sr26.56	96-154-0864	0.6656
	Ag92 Al92 H96 O432 Si100	96-152-6854	0.6654
	A92 H306 N102 O384 Si100 Sr46	96-152-1406	0.6648
	A96 D53.3952 Na36.704 O453.093 Si96	96-152-2337	0.6648
	A86.016 Cr4.192 Na54.016 O396.192 Si105.984	96-152-5063	0.6643

K54.7 Al54.7 Si137.3 O384 (N H4)10.7 (N C H3)4)3.33 (Sm4 (Mo O4) (H2 O)16 (Mo7 O24)4) (H2 O)22C13.32 H158.76 Mo29 N14.03 O138 Sm4 and 267 others...	C8 H24 Cd Cl4 N2 Al54.7 K54.7 O384 Si137.3	96-200-0748 96-153-1895 96-403-1606	0.6636 0.6622 0.6618
---	---	---	----------------------------

Search-Match

Settings

Reference database used	COD-Inorg REV218120 2019.09.10
Automatic zero point adaptation	Yes
Minimum figure-of-merit (FoM)	0.60
2theta window for peak corr.	0.30 deg.
Minimum rel. int. for peak corr.	1
Parameter/influence 2theta	0.50
Parameter/influence intensities	0.50
Parameter multiple/single phase(s)	0.50

Criteria for entries added by user

Reference:

Entry number: 96-101-1153;96-300-0049;96-900-8041;96-900-8298;96-900-8732;96-901-4436;96-100-8767;96-100-8768;96-100-8769;96-101-1088;96-221-1653;96-900-2159;96-900-2160;96-900-3077;96-900-3078;96-900-3079;96-900-3080;96-900-3081;96-901-0407;96-901-0408;96-901-0409;96-901-0410;96-901-0411;96-901-1413;96-901-5697;96-901-6060;96-901-6179;96-901-6407;96-101-1082;96-120-0017;96-154-4376;96-900-3875;96-900-8238;96-901-1748;96-901-5516;96-901-5977;96-101-1098;96-101-1160;96-101-1173;96-101-1177;96-101-1201;96-110-0020;96-500-0036;96-900-0776;96-900-0777;96-900-0778;96-900-0779;96-900-0780;96-900-0781;96-900-5018;96-900-5019;96-900-5020;96-900-5021;96-900-5022;96-900-5023;96-900-5024;96-900-5025;96-900-5026;96-900-5027;96-900-5028;96-900-5029;96-900-5030;96-900-5031;96-900-5032;96-900-5033;96-900-5034;96-900-7379;96-900-8093;96-900-8094;96-900-9667;96-901-0145;96-901-0146;96-901-0147;96-901-1494;96-901-1495;96-901-1496;96-901-1497;96-901-2601;96-901-2602;96-901-2603;96-901-2604;96-901-2605;96-901-2606;96-901-3322;96-901-5023;96-900-0849;96-900-1092;96-900-1093;96-900-1639;96-900-1640;96-900-1779;96-900-1883;96-900-4509;96-900-4510;96-900-4511;96-900-4512;96-900-4513;96-900-4514;96-900-4994;96-900-4995;96-900-7425;96-901-4665;96-901-5164;96-901-5487;96-901-5581;96-901-6051;96-901-6148;96-110-1055;96-900-2780;96-901-0957;96-901-0958;96-901-0959;96-901-0960

Peak List

No.	2theta [°]	d [Å]	I/I0	FWHM	Matched
1	5.88	15.0309	102.49	0.5689	E
2	8.90	9.9362	22.79	0.5689	
3	9.58	9.2323	17.89	0.9760	B
4	11.28	7.8445	27.74	0.9760	
5	11.98	7.3876	28.76	0.9760	E
6	14.12	6.2724	14.10	0.1790	
7	16.44	5.3921	22.99	0.1717	
8	18.70	4.7453	20.19	0.2614	D
9	19.68	4.5111	88.49	0.6494	B,E
10	20.96	4.2384	245.42	0.5028	A,B,E
11	24.88	3.5788	29.05	0.2336	D
12	25.82	3.4506	17.87	0.2056	
13	26.70	3.3389	1000.00	0.2708	A,C,E,F
14	28.56	3.1255	25.43	0.3508	F
15	31.20	2.8668	30.26	0.2111	B,D,E
16	33.16	2.7017	38.25	0.4173	C,D,F
17	34.78	2.5795	45.21	0.5922	B,C
18	35.72	2.5137	90.38	0.5922	C,E,F
19	36.58	2.4566	229.22	0.5126	A,B,C,E,F
20	39.50	2.2814	69.77	0.2581	A,B,C,E,F
21	40.36	2.2348	51.54	0.4524	A,B,C,D,E,F
22	42.50	2.1271	53.19	0.2678	A,B,D,E
23	44.52	2.0352	30.85	0.5240	B,F
24	45.82	1.9804	55.43	0.2206	A,B,F
25	50.16	1.8187	151.51	0.2620	A,B,C
26	53.56	1.7110	45.46	0.3320	B,C
27	54.96	1.6707	48.06	0.4021	A,B,D,E,F
28	58.94	1.5670	47.09	0.2635	B,D,F
29	60.00	1.5419	94.06	0.2835	A,B,E,F
30	61.40	1.5100	48.67	0.7223	B,C,E,F
31	67.72	1.3837	35.72	1.1971	A,B,C,F
32	68.32	1.3730	95.16	0.4792	A,B,C,D,F

Integrated Profile Areas

Based on calculated profile

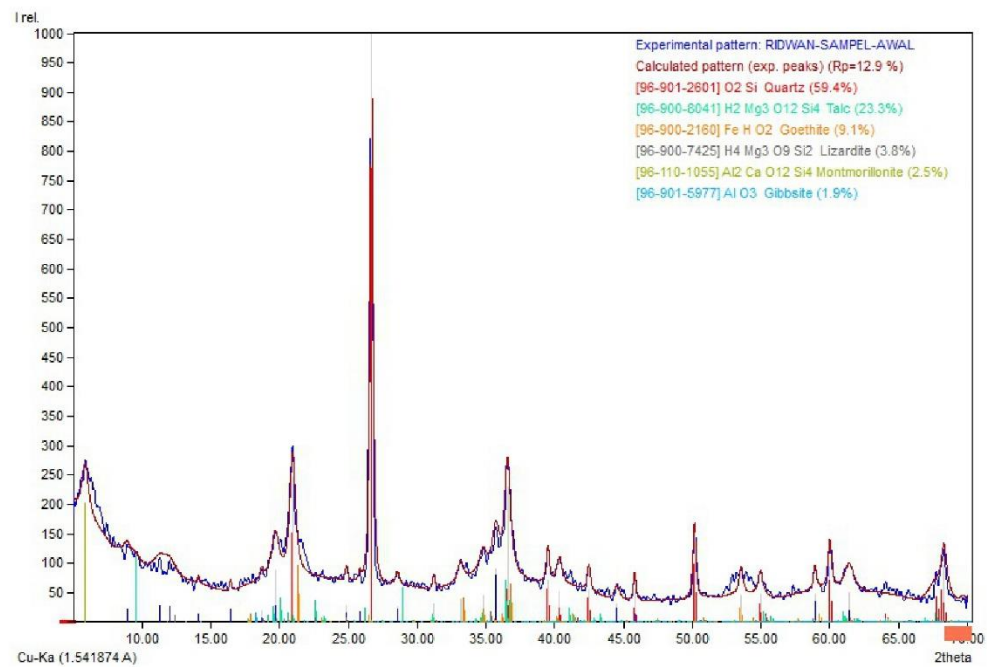
Profile area	Counts	Amount
Overall diffraction profile	111449	100.00%
Background radiation	84967	76.24%
Diffraction peaks	26482	23.76%
Peak area belonging to selected phases	18774	16.85%
Peak area of phase A (Quartz)	9830	8.82%
Peak area of phase B (Talc)	4011	3.60%
Peak area of phase C (Goethite)	2421	2.17%
Peak area of phase D (Lizardite)	452	0.41%
Peak area of phase E (Montmorillonite)	1770	1.59%
Peak area of phase F (Gibbsite)	290	0.26%
Unidentified peak area	7708	6.92%

Peak Residuals

Peak data	Counts	Amount
-----------	--------	--------

Overall peak intensity	514	100.00%
Peak intensity belonging to selected phases	479	93.19%
Unidentified peak intensity	35	6.81%

Diffraction Pattern Graphics



Match! Phase Analysis Report

Sample: RIDWAN-ROASTING-500

Sample Data

File name	RIDWAN-ROASTING-500.txt
File path	D:/TUGAS AKHIR (TA)/HASIL ANALISIS DAN PENGOLAHAN DATA/HASIL ANALISIS/ANALISIS XRD 2/RIDWAN-ROASTING-500
Data collected	Aug 5, 2024 23:16:18
Data range	5.000° - 70.000°
Original data range	5.000° - 70.000°
Number of points	3251
Step size	0.020
Rietveld refinement converged	No
Alpha2 subtracted	No
Background subtr.	No
Data smoothed	Yes
Radiation	X-rays
Wavelength	1.541874 Å

Matched Phases

Index	Amount (%)	Name
A	58.8	Quartz
B	17.7	Hematite-proto
C	9.3	Talc
D	7.7	Montmorillonite
E	5.9	Lizardite
F	0.7	Spinel
	6.7	Unidentified peak area

Formula sum
O2 Si
Fe1.76 H0.06 O3
H2 Mg3 O12 Si4
Al0.86 Fe0.1 H Li0.08 Mg0.14 O10 Si3.9
H4 Mg3 O9 Si2
Al2 Mg O4

A: Quartz (58.8 %)

Formula sum	O2 Si
Entry number	96-900-0776
Figure-of-Merit (FoM)	0.871609
Total number of peaks	70
Peaks in range	36
Peaks matched	30
Intensity scale factor	0.71
Space group	P 32 2 1 S
Crystal system	trigonal (hexagonal axes)
Unit cell	a= 4.9160 Å c= 5.4054 Å
I/lc	3.30
Calc. density	2.646 g/cm³
Reference	Leven L., Prewitt C. T., Weidner D. J., "Structure and elastic properties of quartz at pressure P = 1 atm", American Mineralogist 65 , 920-930 (1980)

B: Hematite-proto (17.7 %)

Formula sum	Fe1.76 H0.06 O3
Entry number	96-900-2161
Figure-of-Merit (FoM)	0.692881
Total number of peaks	68
Peaks in range	28
Peaks matched	12
Intensity scale factor	0.16
Space group	R-3 c
Crystal system	trigonal (hexagonal axes)
Unit cell	a= 5.0145 Å c= 13.6920 Å
I/lc	2.50
Calc. density	4.890 g/cm³
Reference	Gualtieri A., Venturelli P., "In situ study of the goethite-hematite phase transformation by real times synchrotron powder diffraction Sample at T = 313 C", American Mineralogist 84 , 895-904 (1999)

C: Talc (9.3 %)

Formula sum	H2 Mg3 O12 Si4
Entry number	96-900-8041
Figure-of-Merit (FoM)	0.453376
Total number of peaks	596
Peaks in range	359
Peaks matched	85
Intensity scale factor	0.04
Space group	C 1 2/c 1
Crystal system	monoclinic
Unit cell	a= 5.2600 Å b= 9.1000 Å c= 18.8100 Å β= 100.000 °
I/lc	1.23
Calc. density	2.841 g/cm³
Reference	Gruner J. W., "The crystal structures of talc and pyrophyllite Locality: Harford County, Maryland, USA", Zeitschrift fur Kristallographie 88 , 412-419 (1934)

D: Montmorillonite (7.7 %)

Formula sum	Al0.86 Fe0.1 H Li0.08 Mg0.14 O10 Si3.9
Entry number	96-901-0959
Figure-of-Merit (FoM)	0.763383
Total number of peaks	498
Peaks in range	201
Peaks matched	53
Intensity scale factor	0.17

Space group	C 1 2/m 1		
Crystal system	monoclinic		
Unit cell	a= 5.1710 Å b= 8.9570 Å c= 9.7400 Å β= 96.100 °		
I/lc	5.90		
Calc. density	2.245 g/cm³		
Reference	Gourmis D., Lappas A., Karakassides M. A., Tabbens D., Moukarika A., "Aneutron diffraction study of alkali cation migration in montmorillonites Sample: Li-mont-300", Physics and Chemistry of Minerals 35 , 49-58 (2008)		
E: Lizardite (5.9 %)			
Formula sum	H4 Mg3 O9 Si2		
Entry number	96-900-7425		
Figure-of-Merit (FoM)	0.301446		
Total number of peaks	118		
Peaks in range	55		
Peaks matched	19		
Intensity scale factor	0.03		
Space group	P 1		
Crystal system	triclinic (anorthic)		
Unit cell	a= 5.4340 Å b= 5.4340 Å c= 7.1530 Å α= 90.000° β= 90.000° γ= 120.000°		
I/lc	1.22		
Calc. density	2.516 g/cm³		
Reference	Auzende A. L., Pellenq R. J. M., Devouard B., Baronnet A., Grauby O., "Atomistic calculations of structural and elastic properties of serpentine minerals: the case of lizardite Note: 1T polytype Note: Hypothetical structure derived using semi-empirical potentials", Physics and Chemistry of Minerals 33 , 266-275 (2006)		
F: Spinel (0.7 %)			
Formula sum	Al2 Mg O4		
Entry number	96-900-2864		
Figure-of-Merit (FoM)	0.370625		
Total number of peaks	62		
Peaks in range	18		
Peaks matched	9		
Intensity scale factor	0.00		
Space group	F d -3 m		
Crystal system	cubic		
Unit cell	a= 7.8468 Å		
I/lc	1.77		
Calc. density	3.912 g/cm³		
Reference	Levy D., Pavese A., Hanfland M., "Synthetic MgAl2O4 (spinel) at high pressure conditions (0.0001-30 GPa): Asynchrotron X-ray powder diffraction study P= 22.6 GPa", American Mineralogist 88 , 93-98 (2003)		
Candidates			
Name	Formula	Entry No.	FoM
((Bi Se)1.09 Ta Se2).917	Bi Se	96-210-6936	0.6795
	Lu Ni2 Sn	96-152-2916	0.6760
Sylvite	Cl K	96-900-8652	0.6750
	Ga Pd2 Sc	96-152-3492	0.6744
	Cl K0.8 Na0.2	96-900-3165	0.6735
	Cl K0.7 Na0.3	96-900-3182	0.6729
Sylvite	Cl K	96-900-3114	0.6724
Sylvite	Cl K	96-900-3130	0.6711
	Ta Tc	96-152-7278	0.6701
Calcium	Ca	96-901-2733	0.6691
	Pd Ti	96-152-3470	0.6689
Caesium hydrogenselenide - at 473K	Cs H Se	96-101-0911	0.6684
	Cs Se	96-901-4494	0.6684
	Ni2 Sn Yb	96-152-2918	0.6682
Sylvite	Cl K	96-900-3125	0.6681
(Eu Yb)	Eu Yb	96-152-4623	0.6680
Sylvite	Cl K	96-900-3139	0.6659
	Cl K0.8 Na0.2	96-900-3154	0.6642
Sylvite	Cl K	96-900-3115	0.6638
Potassium	K	96-901-1977	0.6631
	F15 Mo5 O15 Rb15	96-450-8553	0.6630
Rb3 Fe F6	Co Hf	96-152-5531	0.6606
	F6 Fe Rb3	96-152-9655	0.6583
	Cl K0.8 Na0.2	96-900-3160	0.6581
	Cl K0.7 Na0.3	96-900-3183	0.6581
Ag (Mg0.2 Zn0.8)	Ag Mg0.2 Zn0.8	96-150-9453	0.6563
Sylvite	Cl K	96-900-3120	0.6559
Calcium	Ca	96-901-1035	0.6543
	Au Zn	96-151-0323	0.6538
Sylvite	Cl K	96-900-3116	0.6533
Sylvite	Cl K	96-900-3121	0.6533
Sylvite	Cl K	96-900-3135	0.6532
Sylvite	Cl K	96-900-3131	0.6531
Sylvite	Cl K	96-900-9734	0.6530
Sylvite	Cl K	96-900-3113	0.6528
Potassium chloride (Sylvine)	Cl K	96-101-1128	0.6526
	Mg Pd	96-153-8007	0.6525
	Cl K0.8 Na0.2	96-900-3150	0.6521
(H3 O)2 Ni O2	H0.6 Ni O2.2	96-153-4271	0.6514
	Cl K0.7 Na0.3	96-900-3181	0.6514
Li6 N Br3	Br3 Li6 N	96-152-8849	0.6510
Li Ag2 Ge	Ag2 Ge Li	96-150-9810	0.6509
	Sn Te	96-153-9754	0.6488
(Sn0.95 Zn0.05) (Se0.05 Te0.95)	Se0.05 Sn0.95 Te0.95 Zn0.0596-152-7312	0.6462	
	Mn2 Sn W	96-152-3151	0.6461
(Tb0.35 Te0.65)	Tb0.35 Te0.65	96-152-7221	0.6448

(Ga0.039 Sn0.942) Te	Ga0.039 Sn0.942 Te	96-152-3198	0.6445
	Ni Sb Tb	96-153-7830	0.6438
	Sn Te	96-403-1784	0.6435
(Sn0.97 Zn0.03) (S0.03 Te0.97)	S0.03 Sn0.97 Te0.97 Zn0.03	96-152-7311	0.6434
(Sn0.966 Mn0.034) Te	Mn0.034 Sn0.966 Te	96-800-0212	0.6431
	Nd Te	96-153-8863	0.6427

and 1036 others...

Search-Match

Settings

Reference database used	COD-Inorg REV218120 2019.09.10
Automatic zeroipot adaptation	Yes
Minimum figure-of-merit (FoM)	0.60
2theta window for peak corr.	0.30 deg.
Minimum rel. int. for peak corr.	1
Parameter/influence 2theta	0.50
Parameter/influence intensities	0.50
Parameter multiple/single phase(s)	0.50

Criteria for entries added by user

Reference:

Entry number:

901-4718;96-901-4743;96-901-4822;96-901-4829;96-901-4832;96-901-4897;96-901-4924;96-901-4960;96-901-4990;96-901-4991;96-901-5021;96-901-5052;96-901-5110;96-901-5180;96-901-5184;96-901-5203;96-901-5219;96-901-5257;96-901-5273;96-901-5292;96-901-5305;96-901-5353;96-901-5367;96-901-5430;96-901-5450;96-901-5471;96-901-5515;96-901-5540;96-901-5552;96-901-5578;96-901-5590;96-901-5627;96-901-5648;96-901-5665;96-901-5706;96-901-5710;96-901-5717;96-901-5760;96-901-5783;96-901-5846;96-901-5931;96-901-5947;96-901-5972;96-901-6005;96-901-6008;96-901-6022;96-901-6030;96-901-6052;96-901-6077;96-901-6091;96-901-6097;96-901-6176;96-901-6239;96-901-6268;96-901-6317;96-901-6329;96-901-6337;96-901-6344;96-901-6363;96-901-6364;96-901-6365;96-901-6371;96-901-6417;96-901-6435;96-901-6475;96-901-6505;96-901-6565;96-901-6677;96-901-6699;96-901-6720;96-101-1241;96-101-1268;96-210-8028;96-210-8029;96-591-0083;96-900-0140;96-900-2161;96-900-2162;96-900-2163;96-900-9783;96-901-4881;96-901-5066;96-901-5504;96-901-5965;96-901-6458;96-900-0849;96-900-1092;96-900-1093;96-900-1639;96-900-1640;96-900-1779;96-900-1883;96-900-4509;96-900-4510;96-900-4511;96-900-4512;96-900-4513;96-900-4514;96-900-4994;96-900-4995;96-900-7425;96-901-4665;96-901-5164;96-901-5487;96-901-5581;96-901-6051;96-901-6148;96-110-1055;96-900-2780;96-901-0957;96-901-0958;96-901-0959;96-901-0960;96-154-4616;96-154-4617;96-900-0167;96-900-0168;96-900-0268;96-900-0315;96-900-0316;96-900-0317;96-900-0318;96-900-0319;96-900-0320;96-900-0321;96-900-0322;96-900-0323;96-900-0324;96-900-0325;96-900-0326;96-900-0327;96-900-0535;96-900-0536;96-900-0537;96-900-0538;96-900-0539;96-900-0540;96-900-0541;96-900-0542;96-900-0788;96-900-1667;96-900-1668;96-900-1669;96-900-1670;96-900-1671;96-900-4323;96-900-4324;96-900-4325;96-900-4326;96-900-4327;96-900-4328;96-900-4329;96-900-4330;96-900-4331;96-900-4332;96-900-4333;96-900-7378;96-901-0755;96-901-0756;96-901-0757;96-901-0758;96-901-0759;96-901-0760;96-901-0761;96-901-0762;96-901-0763;96-901-0764;96-901-0765;96-901-0766;96-901-0776;96-901-0777;96-901-0778;96-901-0779;96-901-0780;96-901-0781;96-901-1462;96-901-1463;96-901-1464;96-901-1465;96-901-1466;96-901-1467;96-901-1468;96-901-3094;96-901-3095;96-901-3096;96-901-3097;96-901-3098;96-901-3099;96-901-3100;96-901-3101;96-901-3102;96-901-3640;96-901-3641;96-901-3642;96-901-4298;96-901-5075;96-901-5346;96-901-5659;96-901-6386;96-900-0048;96-101-1019;96-154-5543;96-154-8550;96-154-8551;96-154-8552;96-900-1179;96-900-1221;96-900-1594;96-900-1595;96-900-1596;96-900-1597;96-900-1598;96-900-1599;96-900-1600;96-900-1601;96-900-1602;96-900-1642;96-900-1643;96-900-1644;96-900-1645;96-900-1646;96-900-1700;96-900-1701;96-900-2711;96-900-2712;96-900-2713;96-900-2714;96-900-2715;96-900-2716;96-900-2717;96-900-4030;96-900-4031;96-900-4032;96-900-4033;96-900-4034;96-900-4118;96-900-4119;96-900-4957;96-900-4958;96-900-5542;96-900-5543;96-900-5544;96-900-5545;96-900-5589;96-900-5590;96-900-5576;96-900-5777;96-900-6338;96-900-6339;96-900-6340;96-900-6341;96-900-6342;96-900-6343;96-900-6437;96-900-6438;96-900-6429;96-900-6430;96-900-6431;96-900-6432;96-900-6433;96-900-6434;96-900-6435;96-900-6436;96-900-6437;96-900-6438;96-900-6439;96-900-6440;96-900-6441;96-900-6442;96-900-6443;96-900-8078;96-900-8165;96-901-0242;96-901-0872;96-901-0873;96-901-0874;96-901-0888;96-901-0889;96-901-0890;96-901-0891;96-901-0892;96-901-0893;96-901-0894;96-901-0895;96-901-0896;96-901-0897;96-901-0898;96-901-0899;96-901-1582;96-901-3659;96-901-4118;96-901-4448;96-901-4536;96-901-4861;96-901-4978;96-901-4984;96-901-5810;96-901-6053;96-901-6154;96-901-6258;96-901-6266;96-901-6573

Peak List

No.	2theta [°]	d [Å]	I/I0	FWHM	Matched
1	7.08	12.4857	37.42	0.3555	
2	9.12	9.6970	67.25	1.2330	D
3	11.96	7.4000	14.11	0.6066	
4	13.36	6.6275	14.84	0.6066	
5	19.70	4.5066	61.93	0.7338	C,D,F
6	20.88	4.2545	203.64	0.3162	A,C,D
7	22.00	4.0404	11.25	0.1705	C,D
8	24.32	3.6599	32.64	0.3288	B,C
9	24.92	3.5732	27.87	0.2285	E
10	26.70	3.3389	1000.00	0.2697	A
11	28.24	3.1602	50.46	0.7403	D
12	31.16	2.8704	8.94	0.3268	C,E
13	32.26	2.7750	24.26	0.3068	F
14	33.18	2.7001	58.71	0.7309	B,E
15	35.78	2.5096	128.78	1.2837	B,D
16	36.64	2.4527	161.87	0.6446	A,C,D
17	39.52	2.2803	86.30	0.3128	A,B,C,F
18	40.34	2.2359	65.10	0.4085	A,C,D,E
19	42.48	2.1280	78.10	0.2211	A,C,D,E
20	44.74	2.0257	20.21	0.3620	C
21	45.84	1.9796	44.69	0.3091	A,C,D
22	49.66	1.8359	27.57	0.6808	B,C,D
23	50.20	1.8174	179.38	0.2441	A,C
24	54.06	1.6964	47.49	0.7016	B,C,D
25	54.90	1.6724	59.92	0.7016	A,C,D,E
26	57.30	1.6079	12.10	0.7016	A,C,D,F
27	58.94	1.5670	29.15	0.2912	C,D,E
28	60.00	1.5419	107.23	0.2776	A,C,D
29	61.24	1.5136	28.48	0.4844	C,D,F
30	64.08	1.4532	63.69	0.4585	A,B,C,D
31	64.98	1.4352	58.68	0.3371	C,D,E
32	67.78	1.3826	50.56	0.7085	A,C,D,F
33	68.34	1.3726	81.52	0.6605	A,C,D,E

Integrated Profile Areas

Based on calculated profile

Profile area	Counts	Amount
Overall diffraction profile	105039	100.00%
Background radiation	81724	77.80%
Diffraction peaks	23315	22.20%
Peak area belonging to selected phases	16227	15.45%
Peak area of phase A (Quartz)	8836	8.41%
Peak area of phase B (Hematite-proto)	3160	3.01%
Peak area of phase C (Talc)	1537	1.46%
Peak area of phase D (Montmorillonite)	2016	1.92%
Peak area of phase E (Lizardite)	599	0.57%
Peak area of phase F (Spinel)	79	0.07%
Unidentified peak area	7088	6.75%

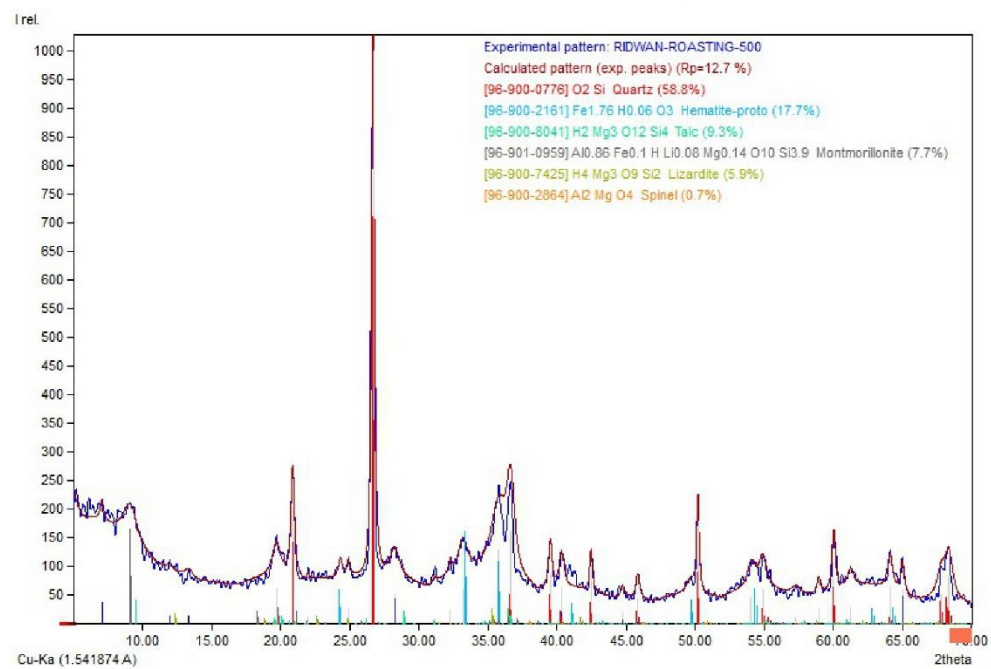
Peak Residuals

Peak data	Counts	Amount
-----------	--------	--------

Overall peak intensity
Peak intensity belonging to selected phases
Unidentified peak intensity

528 100.00%
513 97.19%
15 2.81%

Diffraction Pattern Graphics



Match! Copyright © 2003-2019 CRYSTAL IMPACT, Bonn, Germany

Match! Phase Analysis Report

Sample: RIDWAN-RESIDU-500

Sample Data

File name	RIDWAN-RESIDU-500.txt
File path	D:/TUGAS AKHIR (TA)/HASIL ANALISIS DAN PENGOLAHAN DATA/HASIL ANALISIS/ANALISIS XRD 2/RIDWAN-RESIDU-500
Data collected	Aug 5, 2024 23:16:18
Data range	5.000° - 70.000°
Original data range	5.000° - 70.000°
Number of points	3251
Step size	0.020
Rietveld refinement converged	No
Alpha2 subtracted	No
Background subtr.	No
Data smoothed	Yes
Radiation	X-rays
Wavelength	1.541874 Å

Matched Phases

Index	Amount (%)	Name
A	83.9	Quartz
B	6.6	Talc
C	5.3	Spinel
D	2.3	Lizardite
E	1.6	Hematite-proto
F	0.3	Montmorillonite
	5.0	Unidentified peak area

Formula sum
O2 Si
H2 Mg3 O12 Si4
Al2 Mg O4
H4 Mg3 O9 Si2
Fe1.76 H0.06 O3
Al0.86 Cs0.08 Fe0.1 H Mg0.14 O10 Si3.9

A: Quartz (83.9 %)

Formula sum	O2 Si
Entry number	96-901-2601
Figure-of-Merit (FoM)	0.880382
Total number of peaks	70
Peaks in range	36
Peaks matched	28
Intensity scale factor	0.63
Space group	P 31 2 1
Crystal system	trigonal (hexagonal axes)
Unit cell	a= 4.9140 Å c= 5.4060 Å
I/c	3.32
Calc. density	2.648 g/cm³
Reference	Hazen R. M., Finger L. W., Hemley R. J., Mao H. K., "High-pressure crystal chemistry and amorphization of alpha-quartzLocality: syntheticSample: P = 1 bar", Solid State Communications 72 , 507-511 (1989)

B: Talc (6.6 %)

Formula sum	H2 Mg3 O12 Si4
Entry number	96-900-8041
Figure-of-Merit (FoM)	0.464472
Total number of peaks	596
Peaks in range	359
Peaks matched	74
Intensity scale factor	0.02
Space group	C 1 2/c 1
Crystal system	monoclinic
Unit cell	a= 5.2600 Å b= 9.1000 Å c= 18.8100 Å β= 100.000 °
I/c	1.23
Calc. density	2.841 g/cm³
Reference	Gruner J. W., "The crystal structures of talc and pyrophylliteLocality: Harford County, Maryland, USA", Zeitschrift fur Kristallographie 88 , 412-419 (1934)

C: Spinel (5.3 %)

Formula sum	Al2 Mg O4
Entry number	96-900-2047
Figure-of-Merit (FoM)	0.549312
Total number of peaks	66
Peaks in range	20
Peaks matched	10
Intensity scale factor	0.02
Space group	F d -3 m
Crystal system	cubic
Unit cell	a= 8.1114 Å
I/c	1.86
Calc. density	3.541 g/cm³
Reference	Redfern S. A. T., Harrison R. J., O'Neill H St C, Wood D. R. R., "Thermodynamics and kinetics of cation ordering in MgAl2O4 spinel up to 1600 Cfrom in situ neutron diffraction Data collected at IPNS, Argonne NationalLaboratory, T = 707 K on heating cycle, MgAl2O4", American Mineralogist 84 , 299-310 (1999)

D: Lizardite (2.3 %)

Formula sum	H4 Mg3 O9 Si2
Entry number	96-900-1640
Figure-of-Merit (FoM)	0.335348
Total number of peaks	118
Peaks in range	56
Peaks matched	17
Intensity scale factor	0.01

Space group	P 3 1 m
Crystal system	trigonal (hexagonal axes)
Unit cell	a= 5.3380 Å c= 7.2570 Å
I/lc	1.42
Calc. density	2.570 g/cm ³
Reference	Mellini M, Viti C., "Crystal structure of lizardite-1T from Elba, Italy Sample: MFN3-6 Note:U(1,2) for Si, O2 and O4 have been changed to match symmetry constraints.", American Mineralogist 79 , 1194-1198 (1994)

E: Hematite-proto (1.6 %)

Formula sum	Fe1.76 H0.06 O3
Entry number	96-900-2161
Figure-of-Merit (FoM)	0.294276
Total number of peaks	68
Peaks in range	28
Peaks matched	5
Intensity scale factor	0.01
Space group	R -3 c
Crystal system	trigonal (hexagonal axes)
Unit cell	a= 5.0145 Å c= 13.6920 Å
I/lc	2.50
Calc. density	4.890 g/cm ³
Reference	Gualtieri A, Venturelli P, "In situ study of the goethite-hematite phase transformation by real timesynchrotron powder diffraction Sample at T = 313 °C", American Mineralogist 84 , 895-904 (1999)

F: Montmorillonite (0.3 %)

Formula sum	Al0.86 Cs0.08 Fe0.1 H Mg0.14 O10 Si3.9
Entry number	96-901-0958
Figure-of-Merit (FoM)	0.282378
Total number of peaks	602
Peaks in range	258
Peaks matched	37
Intensity scale factor	0.01
Space group	C 1 2/m 1
Crystal system	monoclinic
Unit cell	a= 5.1810 Å b= 8.9450 Å c= 12.3400 Å β= 99.620 °
I/lc	9.23
Calc. density	1.846 g/cm ³
Reference	Gournis D., Lappas A., Karakassis M. A., Tobbens D., Moukarika A, "Aneutron diffraction study of alkali cation migration in montmorillonites Sample: Cs-mont", Physics and Chemistry of Minerals 35 , 49-58 (2008)

Candidates

Name	Formula	Entry No.	FoM
Quartz	O2 Si	96-900-5018	0.7150
Quartz	O2 Si	96-901-3322	0.7149
Silicon oxide \$-alpha (Quartz low)	O2 Si	96-101-1098	0.7148
	O2 Si	96-230-0371	0.7135
	O2 Si	96-710-3015	0.7128
Quartz	O2 Si	96-901-0146	0.7122
Silicon oxide (Quartz)	O2 Si	96-500-0036	0.7109
Silicon oxide \$-alpha (Quartz low)	O2 Si	96-101-1173	0.7107
Quartz	O2 Si	96-901-2601	0.7099
Quartz	O2 Si	96-900-9667	0.7096
	O2 Si	96-210-0189	0.7094
Quartz	O2 Si	96-900-0776	0.7083
Si O2	O2 Si	96-152-6861	0.7079
Quartz	O2 Si	96-901-0147	0.7079
Quartz	O2 Si	96-901-1494	0.7061
Quartz	O2 Si	96-900-5019	0.7034
Si O2	O2 Si	96-153-2513	0.6997
Silicon oxide (Quartz low)	O2 Si	96-101-1160	0.6961
Quartz	O2 Si	96-901-0145	0.6960
	Be F2	96-153-1932	0.6936
Silicon oxide - \$-alpha (Quartz low)	O2 Si	96-101-1177	0.6921
Quartz	O2 Si	96-900-5020	0.6871
Si O2	O2 Si	96-153-8065	0.6782
Berlineite	Al O4 P	96-900-6550	0.6777
Graphite	C	96-901-2231	0.6774
Graphite	C	96-901-1578	0.6762
Graphite	C	96-900-8570	0.6636
Quartz	O2 Si	96-900-5021	0.6634
Graphite	C	96-900-0047	0.6631
Coquimbite	Al1.05 Fe2.942 H36 O42 S696-900-5752	0.6602	
Al P O4	Al O4 P	96-153-0003	0.6586
	C7 H14 Cl N O5	96-723-1664	0.6552
Coquimbite	Al0.9 Fe3.1 H36 O42 S6	96-900-0207	0.6547
	B N	96-900-8998	0.6464
Boron Nitride	B N	96-591-0080	0.6449
Al P O4	Al O4 P	96-231-0665	0.6403
Hydrogen	H2	96-901-3092	0.6395
	Al0.05 Li0.05 O2 Si0.95	96-900-2384	0.6389
Quartz	O2 Si	96-901-5023	0.6357
Manganese Oxide (2.03/4)	Mn2.03 O4	96-151-4234	0.6350
Lithium Manganese Oxide (0.2/1.9/4)	Li0.2 Mn1.9 O4	96-151-4078	0.6349
hexagonal boron nitride	B N	96-201-6171	0.6343
Hg (S0.4 Se0.6)	Hg S0.4 Se0.6	96-152-1789	0.6337
Berlineite	Al O4 P	96-900-6549	0.6327
Coquimbite	Al Fe3 H36 O42 S6	96-901-6274	0.6279
Coquimbite	Al Fe3 H36 O42 S6	96-901-5119	0.6278
	Ti V	96-154-1238	0.6268

Quartz	O2 Si	96-900-5022	0.6260
	Cs Fe O6 Si2	96-201-0089	0.6253
(Mo0.666 Ti0.167 Zr0.167)	Mo0.666 Ti0.167 Zr0.167	96-152-3265	0.6250
(Mo0.875 Zr0.125)	Mo0.875 Zr0.125	96-152-2702	0.6249
Tungsten	W	96-900-6510	0.6245
and 808 others...			

Search-Match

Settings

Settings Reference database used COD-Inorg REV218120 2019.09.10
 Automatic zero point adaptation Yes
 Minimum figure-of-merit (FoM) 0.60
 2theta window for peak corr. 0.30 deg.
 Minimum rel. int. for peak corr. 1
 Parameter/influence 2theta 0.50
 Parameter/influence intensities 0.50
 Parameter multiple/single phase(s) 0.50

Criteria for entries added by user

Reference:

901-5292;96-901-5305;96-901-5353;96-901-5367;96-901-5430;96-901-5450;96-901-5471;96-901-5515;96-901-5540;96-901-5552;96-901-5578;96-901-5590;96-901-5627;96-901-5648;96-901-5665;96-901-5706;96-901-5710;96-901-5717;96-901-5760;96-901-5783;96-901-5846;96-901-5931;96-901-5947;96-901-5972;96-901-6005;96-901-6008;96-901-6022;96-901-6030;96-901-6052;96-901-6077;96-901-6091;96-901-6097;96-901-6176;96-901-6239;96-901-6268;96-901-6317;96-901-6329;96-901-6337;96-901-6344;96-901-6363;96-901-6364;96-901-6365;96-901-6371;96-901-6417;96-901-6435;96-901-6475;96-901-6505;96-901-6565;96-901-6578;96-901-6603;96-901-6677;96-901-6699;96-901-6720;96-101-1241;96-101-1268;96-210-8028;96-210-8029;96-591-0083;96-900-0140;96-900-2161;96-900-2162;96-900-2163;96-900-9783;96-901-4881;96-901-5066;96-901-5504;96-901-5965;96-901-6458;96-900-0849;96-900-1092;96-900-1093;96-900-1639;96-900-1640;96-900-1779;96-900-1883;96-900-4509;96-900-4510;96-900-4511;96-900-4512;96-900-4513;96-900-4514;96-900-4994;96-900-4995;96-900-7425;96-901-4665;96-901-5164;96-901-5487;96-901-5581;96-901-6051;96-901-6148;96-110-1055;96-900-2780;96-901-0957;96-901-0958;96-901-0959;96-901-0960

Peak List

No.	2theta [°]	d [Å]	I/I₀	FWHM	Matched
1	9.44	9.3689	32.72	0.4661	B
2	10.68	8.2838	24.06	0.3011	
3	15.68	5.6517	12.59	0.1771	
4	16.16	5.4849	15.34	0.4856	
5	18.82	4.7153	12.04	0.7225	C
6	19.42	4.5709	25.27	0.9022	B,D
7	19.74	4.4975	29.66	0.6080	B,F
8	20.88	4.2545	191.43	0.3138	A,B,F
9	22.80	3.9004	11.68	0.3188	B,D,F
10	24.50	3.6335	24.51	0.4675	B,D,E,F
11	25.44	3.5013	13.51	0.3624	B
12	26.68	3.3413	1000.00	0.2796	A,F
13	28.30	3.1536	18.94	0.3076	
14	29.46	3.0320	16.18	0.1916	B,F
15	32.44	2.7600	32.37	0.3293	B
16	35.44	2.5329	17.89	0.5581	B,F
17	36.60	2.4553	142.40	0.2683	A,B,C,F
18	39.50	2.2814	77.41	0.2495	A,B,E
19	40.32	2.2369	39.67	0.2263	A,B,F
20	42.50	2.1271	64.68	0.2613	A,B,D,F
21	44.66	2.0291	19.77	0.2740	B,C,F
22	45.84	1.9796	51.13	0.2390	A,B
23	50.18	1.8181	161.76	0.2432	A,B,D
24	54.90	1.6724	44.80	0.3270	A,B,D,F
25	59.98	1.5423	94.85	0.2874	A,B,D,F
26	64.08	1.4532	20.33	0.2243	A,B,D,E,F
27	64.88	1.4372	24.02	0.3989	B,C,F
28	67.76	1.3830	65.83	0.3317	A,B,D,F
29	68.30	1.3733	84.49	0.4843	A,B,C,F

Integrated Profile Areas

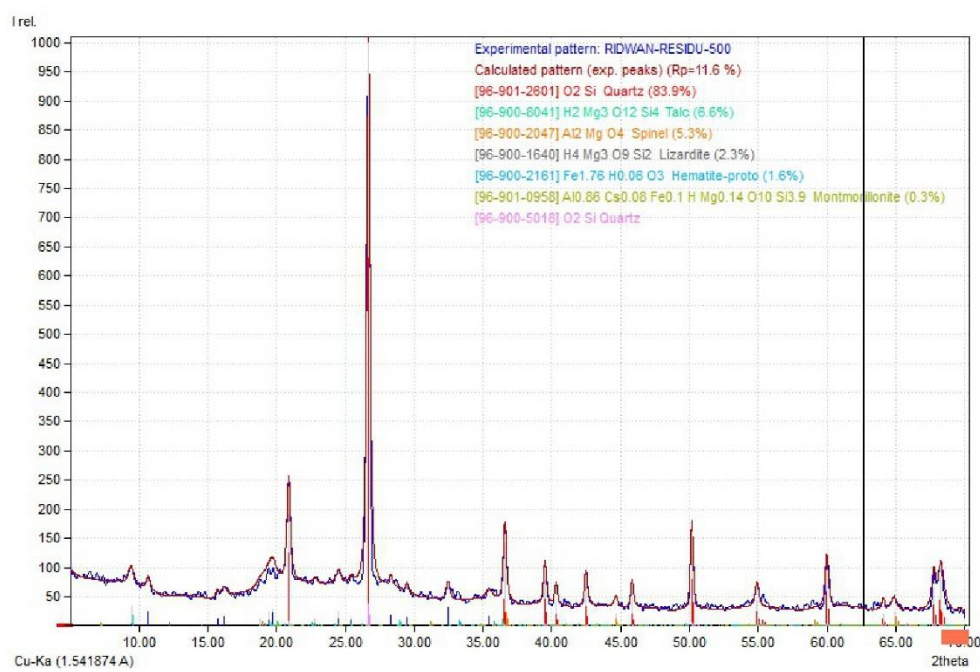
Based on calculated profile

Profile area	Counts	Amount
Overall diffraction profile	147273	100.00%
Background radiation	114040	77.43%
Diffraction peaks	33233	22.57%
Peak area belonging to selected phases	25815	17.53%
Peak area of phase A (Quartz)	21582	14.65%
Peak area of phase B (Talc)	1892	1.28%
Peak area of phase C (Spinel)	1197	0.81%
Peak area of phase D (Lizardite)	527	0.36%
Peak area of phase E (Hematite-proto)	472	0.32%
Peak area of phase F (Montmorillonite)	146	0.10%
Unidentified peak area	7417	5.04%

Peak Residuals

Peak data	Counts	Amount
Overall peak intensity	674	100.00%
Peak intensity belonging to selected phases	626	92.92%
Unidentified peak intensity	48	7.08%

Diffraction Pattern Graphics



Match! Copyright © 2003-2019 CRYSTAL IMPACT, Bonn, Germany

LAMPIRAN 8
KARTU KONSULTASI TUGAS AKHIR

Lampiran B 10
Kartu Konsultasi Tugas Akhir

JUDUL: EFEK PEMANASAN TERHADAP TINGKAT PELINDIAN NIKEL DAN KOBALT DARI BIJIH LIMONIT PULAU KABAENA MENGGUNAKAN ASAM SULFAT

(Konsultasi minimal 8 kali)

TANGGAL	MATERI KONSULTASI	PARAF DOSEN
15/07/2024	- Hasil Analisis AAS	/
19/07/2024	<ul style="list-style-type: none"> - Abstrak - Tujuan dan Manfaat - Hasil Analisis XRD 	/
24/07/2024	<ul style="list-style-type: none"> - Latar Belakang - Petar Pengambilan Sampel - Grafik Tingkat Pelindian 	/
29/07/2024	- Hasil Analisis XRD	/
05/08/2024	<ul style="list-style-type: none"> - Kesimpulan - Daftar Pustaka 	/
12/08/2024	<ul style="list-style-type: none"> - Artikel Ilmiah - Poster 	/
14/08/2024	- Artikel Ilmiah	/

TANGGAL	MATERI KONSULTASI	PARAF DOSEN
12/09/2024	<ul style="list-style-type: none"> - Diagram Alir - Hasil Analisis XRD - Kesimpulan 	
03/10/2024	<ul style="list-style-type: none"> - Penulisan kata "Pemanggangan" - Tambah Saran 	